Relationship between maximal aerobic power with aerobic fitness as a function of signal-to-noise ratio.

*Thomas Beltrame [1,2] beltramethomas@gmail.com, Mariana de Oliveira Gois [1] marigois@yahoo.com.br, Uwe Hoffmann [3] u.hoffmann@dshs-koeln.de, Jessica Koschate [4] Jessica.Koschate@uni-oldenburg.de, Richard Lee Hughson [5] hughson@uwaterloo.ca, Maria Cecília Moraes Frade [1] mariaceciliafrade@gmail.com, Stephanie Nogueira Linares [1] stenolinares@gmail.com, Ricardo da Silva Torres [6] ricardo.torres@ntnu.no, Aparecida Maria Catai [1] mcatai@ufscar.br.

[1] Department of Physical Therapy, Federal University of São Carlos, São Carlos, São Paulo, Brazil.

[2] *Universidade Ibirapuera*, São Paulo, São Paulo, Brazil.

[3] German Sport University Cologne, Cologne, Germany.

[4] Geriatric Medicine, Carl von Ossietzky University Oldenburg, Oldenburg, Germany.

[5] University of Waterloo, Schlegel-University of Waterloo Research Institute for Aging, Waterloo, Ontario, Canada.

[6] Department of ICT and Natural Sciences, Faculty of Information Technology and Electrical Engineering, NTNU - Norwegian University of Science and Technology, Ålesund, Norway.

Reunning Title: Aerobic Power and Fitness

Address for correspondence:

Dr. Thomas Beltrame

Federal University of São Carlos – UFSCar. Rodovia Washington Luís, s/n, São Carlos - SP, Postal code 13565-905, Brazil.

e-mail: beltramethomas@gmail.com

Abstract

Efforts to better understand cardiorespiratory health are relevant for the future development of optimized physical activity programs. We aimed to explore the impact of the signal quality on the expected associations between the ability of the aerobic system in supplying energy as fast as possible during moderate exercise transitions with its maximum capacity to supply energy during maximal exertion. It was hypothesized that a slower aerobic system response during moderate exercise transitions is associated with a lower maximal aerobic power; however, this relationship relies on the quality of the oxygen uptake dataset. Forty-three apparently healthy participants performed a moderate constant work rate (CWR) followed by a pseudorandom binary sequence (PRBS) exercise protocol on a cycle ergometer. Participants also performed a maximum incremental cardiopulmonary exercise testing (CPET). The maximal aerobic power was evaluated by the peak oxygen uptake during the CPET and the aerobic fitness was estimated from different approaches for oxygen uptake dynamics analysis during the CWR and PRBS protocols at different levels of signal-to-noise ratio. The product moment correlation coefficient was used to evaluate the correlation level between variables. Aerobic fitness was correlated with maximum aerobic power, but this correlation increased as a function of the signal-to-noise ratio. Aerobic fitness is related to maximal aerobic power; however, this association appeared to be highly dependent on the data quality and analysis for aerobic fitness evaluation. Our results show that simpler moderate exercise protocols might be as good as maximal exertion exercise protocols to obtain indexes related to cardiorespiratory health.

Keywords: oxygen uptake kinetics, oxygen consumption, cardiorespiratory fitness, exercise.

Acknowledgments: This study was financially supported by São Paulo State Research Foundation - FAPESP (grants 2016/22215-7, 2017/09639-5, and 2018/19016-8), National Council for Scientific and Technological Development - CNPq (grant 311938/2013-2 and 168866/2017-0), and the Coordination for the Improvement of Higher Education Personnel - CAPES (research grant AUXPE 1766732/2018–2021). The funders had no role in study design, data collection and analysis, decision to publish, or preparation of manuscript.

New & Noteworthy

- Optimized methods for cardiorespiratory health evaluation are of great interest for public health.
- Moderate exercise protocols might be as good as maximum exertion exercise protocols to evaluate cardiorespiratory health.
- Pseudorandom or constant workload moderate exercise can be used to evaluate cardiorespiratory health.

1. *Introduction*

Efforts to better assess cardiorespiratory health (CRH) are relevant for the future development of optimized physical activity programs, mainly those designed for chronic diseases that directly affect functional capacity (1, 51), quality of life (39), and mortality (36). In addition, sub-clinical impairments in CRH seem to be related to the onset of chronic diseases (13) that are responsible for 41 million deaths every year (56, 57). Therefore, optimized methods for CRH evaluation are of great interest for public health.

CRH can be investigated through the characterization of maximal aerobic power or aerobic fitness level, and these indexes are related to different aspects of the aerobic system response. Maximal aerobic power is related to the maximum ability of the aerobic system to supply energy (18), thus it is directly related to functional capacity. Experimentally, maximal aerobic power is commonly evaluated during incremental exercise to volitional exhaustion by the measurement of the peak alveolar oxygen uptake ($a\dot{V}O_{2-peak}$) (49). On the other hand, aerobic fitness is related to the speed of the aerobic system response to meet a new energetic demand (50) and it is commonly characterized during constant (11, 27) or pseudorandom (6, 8, 31) moderate work rate exercise protocols. However, the term "aerobic fitness" can be also interpreted as maximal aerobic power, and the speed of the aerobic adjustment during exercise transitions as muscle oxidative capacity (53). Here, the terms "aerobic power" and "aerobic fitness" will be exclusively related to $a\dot{V}O_{2-peak}$ and the alveolar oxygen uptake ($a\dot{V}O_2$) dynamics, respectively. In any manner, the speed of the alveolar oxygen uptake ($a\dot{V}O_2$) response can be estimated in time domain (by the time constant τ), in frequency domain (by indexes, such as the mean normalized gain [MNG]), or by cross-correlation function (by the peak of this function [CCF_{peak}]) (9, 33). The discussion of which one of these indexes is the most appropriate method for aerobic fitness evaluation remains unclear (9, 14, 19, 27).

Despite the expected relationship between maximal aerobic power and fitness, this relationship is rarely reported (6), possibly due to experimental noise introduced by data collection (22, 46) and processing (27). Additionally, the elevated degree of distortion between the local and central hemodynamics during exercise transitions challenges the assumption that the $a\dot{V}O_2$ reflects the muscular aerobic metabolism, potentially leading to misinterpretations of the actual aerobic fitness level based on $a\dot{V}O_2$ data (8, 16, 28). Therefore, specific data analysis methods are necessary for the correct evaluation of the aerobic fitness level from $a\dot{V}O_2$ dynamics data during exercise transitions (9, 27, 42).

Even though characterization of CRH opens the unique possibility to estimate clinical indexes that are related to mortality and quality of life, extraction of these indexes, based on the study of the aerobic system response remains challenging. Risks associated with peak exertion, bad data handling, need for highly trained technicians, too general physiological assumptions, and user adherence, are barriers that need to be overcome. This study evaluated how data quality influences the expected association between maximal aerobic power with aerobic fitness. For this purpose, we explored the impact of the signal quality on the expected associations between the ability of the aerobic system in supplying energy as fast as possible during moderate exercise transitions (aerobic fitness) with its maximum capacity to supply energy during maximal exertion. It is hypothesized that a slower aerobic system response during exercise transitions is associated with a lower peak aerobic power; however, this relationship relies on $a\dot{V}O_2$ signal-to-noise ratio and the method used to evaluate aerobic fitness.

2. Materials and Methods

2.1 Ethics Statement and Study Design

This study was in accordance with the Declaration of Helsinki (1964), it received approval from the local Human Research Ethics Committee (CAAE: 80459817.5.1001.5504) of the Federal University of São Carlos, São Carlos, SP, Brazil, and it was conducted in compliance with the norms that regulate research involving human subjects (Resolution 466 of 2012, Brazilian National Health Council). After agreeing to take part in the study, all participants signed the informed consent statement. The inclusion criterion was men or women aged between 20 to 42 years. The exclusion criteria were diagnosis of cardiovascular, metabolic, neurological, or respiratory disorder; history of skeletal muscle injury in the previous six months; or chronic joint disease.

Data were obtained from forty-three participants (23 men and 20 women, 27±5 years old, 69±11 kg and 170±9 cm) who performed an initial clinical maximal cardiopulmonary exercise testing (CPET), in the presence of a cardiologist, to identify any possible clinical adverse response to maximal exercise including electrocardiogram abnormalities, ischemia, or reactive hypertension. The cycle ergometer increment was calculated according to previous literature (52). All participants were cleared to perform the exercise protocols of this study. During this same visit, the gas exchange threshold (GET) was identified by the *v*-slope method (4) and used for the next laboratory visit. After 7±3 days, participants performed, in sequence, a constant work rate (CWR), the pseudorandom binary sequence (PRBS) and another CPET protocol. More details about each of the exercise protocols are described below in the text. Laboratory temperature and humidity range were maintained constant for all exercise tests (22-24 ºC and 40-60 %, respectively).

2.2 Exercise Protocols

Based on the $\dot{W}$ at the GET (107±30 watts) obtained during the first visit, the CWR protocol was composed of 3 minutes cycling at 20%, followed by 6 minutes at 80% of the $\dot{W}$ at GET (21±5 and 86±23 watts, respectively). For a complete random exercise protocol that changes $\dot{W}$ between two levels, it is likely to observe low energy stimulus at the frequencies of interest (29). Therefore, the design of optimized exercise protocols for frequency domain analysis are necessary. After the CWR protocol, the PRBS protocol with a total duration of 900 s, started by varying the $\dot{W}$ also between 20 and 80% of the GET, and each step had a length of 30 s (23). The sequence of the PRBS steps were obtained by a shift register (Figure 1), as described elsewhere (58), and an extra 150-s PRBS sequence was added between the CWR and PRBS for a better signal stabilization between protocols.

The PRBS protocol that allows the simultaneous test of multiple frequencies (21) were generated by a 4-stage digital shift register (23, 44) that generated 15 30-s units that varied the work rate between two levels (Figure 1).

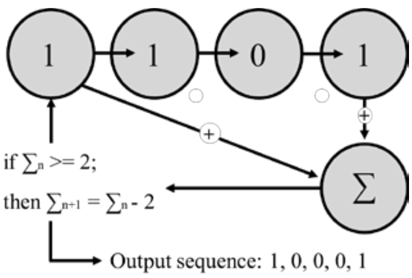

Figure 1. Digital shift register composed by 4 stages to generate pseudorandom binary sequence exercise protocols. The addition feedback module (∑) add the values of the first and the fourth stage and check the criteria statement. This result (0 or 1) is recorded and then inserted into stage 1, and the register is shifted to the right. The output sequence composed by 1 and 0 is transformed in the target work rates where 1 = 80 % and 0 = 20% of the gas exchange threshold.

The shift register was implemented into a computer program to generate the pseudorandom binary sequence exercise protocol. Figure 2 illustrates the program interface.

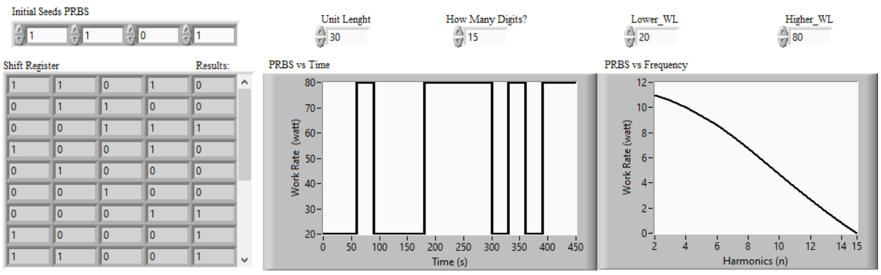

Figure 2. LabVIEW implementation of the digital shift register described in Figure 1 to generate pseudorandom binary sequence (PRBS) exercise protocols. The software has 5 inputs: the number of digits, the unit length, the initial register seeds, and the two work rate levels. From these inputs, the shift register is populated, and the time series of protocol is built. The frequency analysis is also performed to evaluate the signal on frequency space. The inputs are controlled by the user through the program graphical interface and the outputs are also displayed. The exercise protocol on time domain can be exported from the "PRBS vs Time" graph. The software block diagram can be download at: https://doi.org/10.6084/m9.figshare.12206654 (Supplementary Material 1). This software was built on National Instruments LabVIEW Student Edition, 2014, for personal and scientific use only.

After the PRBS protocol, a resting period was performed until the $a\dot{V}O_2$ and pulmonary ventilation ($\dot{V}E$) returned to their baseline values, and another CPET protocol started until physical exhaustion, followed by 6 min of active recovery. The increment of this second CPET was calculated as described in the first CPET. During the CPET, participants were verbally encouraged to give them maximal effort in order to stop the CPET only due to physiologic limitation. Figure 3 displays an example of the exercise protocols and a representative $a\dot{V}O_2$ response to these protocols.

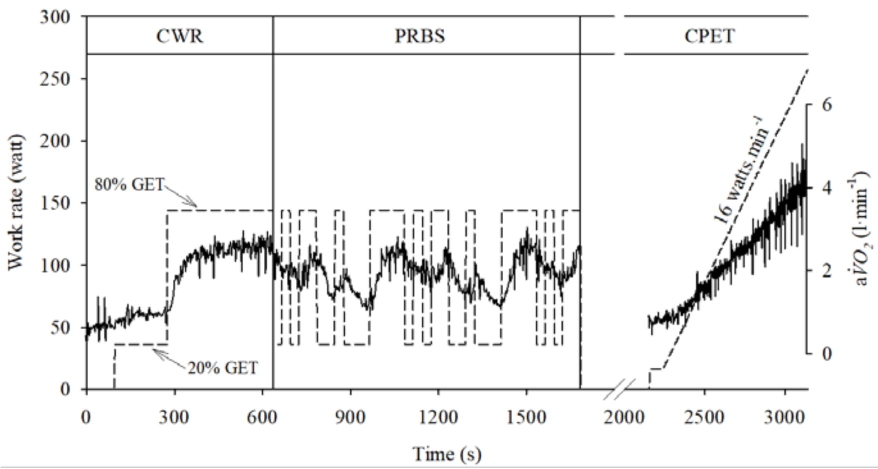

Figure 3. Illustration of the exercise protocols composed of a constant work rate (CWR), a pseudorandom binary sequence (PRBS), and a maximal cardiopulmonary exercise testing (CPET). The two work rates (36 and 144 watts) of the CWR and PRBS protocols corresponded to 20 and 80% of the work rate at the gas exchange threshold (GET) previously identified. The increment rate of the CPET protocol (16 watts.min^{-1} in this case) was calculated accordingly to participant's sex, weight, height, and age. The alveolar oxygen uptake ($a\dot{V}O_2$, in l·min^{-1}) response to these protocols is also plotted.

2.3 Data Collection

During the exercise protocols, the $a\dot{V}O_2$ and $\dot{V}E$ were measured breath-by-breath by a metabolic system (Vmax29c, Sensor Medics, Yorba Linda, CA, USA) calibrated before each experiment. Heart rate (HR) was computed during the exercise based on an ECG system (BioAmp FE132, ADInstruments, Australia).

2.4 Data Analysis

Participant's aerobic fitness was evaluated from the $a\dot{V}O_2$ data during the CWR and PRBS protocols, and their maximal aerobic power was estimated by the $a\dot{V}O_{2-peak}$ during the subsequent CPET. Faster $a\dot{V}O_2$ dynamic responses during the CWR or PRBS protocols were associated with a better aerobic fitness level, and a higher $a\dot{V}O_{2-peak}$ during the CPET was associated with a higher maximal aerobic power level. All data were time synchronized, and second-by-second linearly interpolated by a computer program developed in LabVIEW 2014 (National Instruments, Austin, Texas, USA). For the PRBS protocol, the data of the two complete sequences of 450 s were ensemble averaged to obtain a single PRBS response for each participant.

The aerobic fitness parameter tau (τ, as a time constant) that mostly corresponds to the speed of the muscular aerobic metabolism dynamics (2), was calculated by another LabVIEW 2014 computer routine. This program adjusts the $a\dot{V}O_2$ data during the CWR protocol into a delayed mono-exponential function as previously described (10) using a nonlinear curve fit method that searches for the lowest sum of the squared errors by the standard Levenberg-Marquardt optimization algorithm. As described in Figure 4, by the analysis of the time series response of the error between the fitted function and the interpolated data, the first 18±5 s of data were excluded to eliminate the influences of the cardio-dynamic phase on τ estimation (42). Then, the $a\dot{V}O_2$ data were fitted again into the same function that should be representative of the muscular oxygen uptake dynamics during exercise transition. Since τ is a time constant that quantifies how fast the muscular aerobic metabolism adjusts to a new energetic demand, where lower τ values mean faster responses, this parameter was used to evaluate the aerobic fitness level.

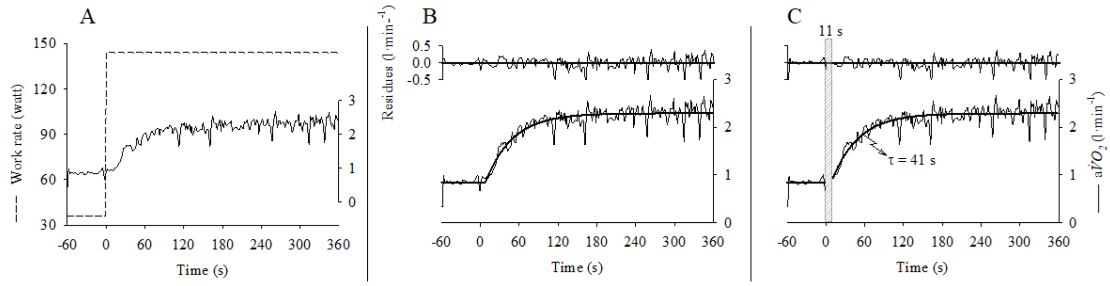

Figure 4. Illustration of the aerobic fitness evaluated by time domain analysis of the alveolar oxygen uptake ($a\dot{V}O_2$) dynamics during exercise transition. The $a\dot{V}O_2$ response to a step exercise protocol (A) is fitted into a delayed mono-exponential model (solid line in B) and the cardiodynamic phase (11 s, fine pattern area in C) is removed from the data by the analysis of the residuals (upper graphs). The remaining $a\dot{V}O_2$ data (C) are fitted into the same exponential model and the time constant τ of this function is obtained. Please see text for more information about data fitting.

Another method to evaluate aerobic fitness was based on frequency domain analysis and focused on the calculation of the MNG index that estimates, as the parameter τ, the speed of the $a\dot{V}O_2$ response during exercise transitions, but during the PRBS protocol. The MNG calculation was already described in previous studies (7, 9). Briefly, the repeated step changes in $\dot{W}$ (forcing function) and the $a\dot{V}O_2$ data were submitted to a discrete fast Fourier transformation to convert the data into frequency space to the maximal frequency of 8.88 mHz where the $\dot{V}O_2$ response follows the linearity principle (21). Afterwards, the system gain ($^{a\dot{V}O_2}/_{\dot{W}}$) for each analyzed frequency was calculated and then normalized as the percentage of the gain at 2.2 mHz. The mean value of the normalized gains of frequencies 4.4, 6.6, and 8.8 mHz was taken as the MNG (in %). Once the $a\dot{V}O_2$ dynamic changes during the PRBS appeared to follow the dynamic linearity principle (21), and most of the response is composed of muscular oxygen uptake (which mean, small cardio-dynamic influences) (23), the MNG can be used to evaluate how fast the aerobic metabolism adjusts during exercise transitions. The MNG varies from 0 to 100% where 0 means no response and values closer to 100 means a dynamic response closer to the forcing function (i.e., instantaneous response). Figure 5 illustrates these calculations for one representative participant.

The aerobic fitness was also evaluated by cross-correlation analysis of the data during the PRBS protocol. In this case, the $a\dot{V}O_2$ data were cross correlated with the forcing function ($\dot{W}$) with a lag time of 1 s, generating a cross-correlation function (CCF) that describes the $a\dot{V}O_2$ dynamic changes as a function of the $\dot{W}$ changes during the PRBS. The peak of this cross-correlation function (CCF_{peak}) is related to the speed of the $a\dot{V}O_2$ to meet a new energetic demand (19), where a peak closer to 1 means a faster response because the $a\dot{V}O_2$ dynamics are closer to the square-like forcing function (instantaneous response). Figure 5 shows an example of the CCF_{peak} calculation.

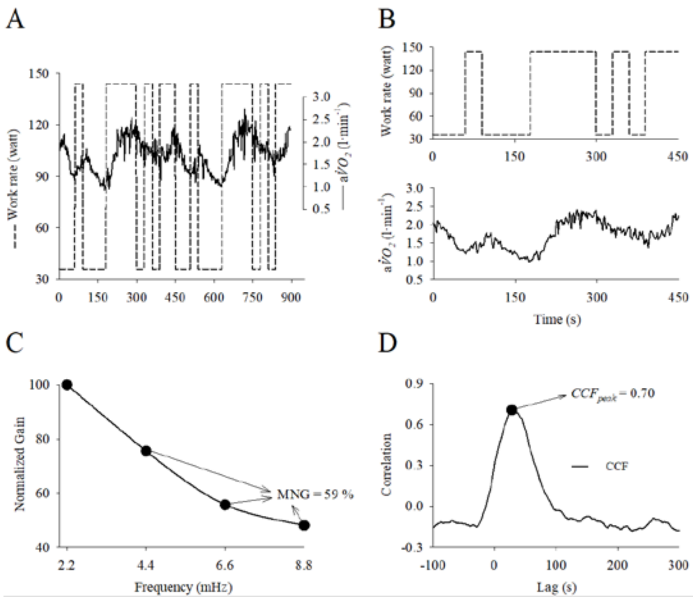

Figure 5. Illustration of the aerobic fitness evaluation based on the analysis of the alveolar oxygen uptake ($a\dot{V}O_2$, solid lines) dynamics during a pseudorandom binary sequence exercise protocol (dashed lines). The second-by-second linearly interpolated data (A) of the two consecutives protocols were ensemble averaged to obtain a single response (B). The exercise protocol and the $a\dot{V}O_2$ were transformed into the frequency space by a fast Fourier transformation and the system gain was calculated by dividing the $a\dot{V}O_2$ by the protocol amplitude at each of the analyzed frequencies and then normalized by the gain at frequency 2.2 mHz. The average of the normalized gains (in %) of the frequencies 4.4, 6.6 and 8.8 mHz (C) was taken as the final index related to aerobic fitness (named Mean Normalized Gain, or MNG). In addition, the exercise protocol work rate (upper graph in B) was cross-correlated with the $a\dot{V}O_2$ response (lower graph in B) accordingly to previous study (19) to obtain the cross-correlation function at different lags. The peak of CCF (CCF_{peak} in D) is also related to the speed of the $a\dot{V}O_2$ dynamics, as the MNG.

Finally, during the CPET, the last 20 s of the $a\dot{V}O_2$ data were averaged to obtain the $a\dot{V}O_{2-peak}$ which was considered as the maximal aerobic power. Since the CPET was performed on cycle ergometer, the $a\dot{V}O_{2-peak}$ was not relativized by body weight to avoid the introduction of a confusion factor in the correlation analyses (49). For the aerobic fitness analysis, the calculated parameters are exclusively related to the response time, so body weight does not influence the data analysis. During the incremental exercise, all participants reached a respiratory exchange ratio (RER) higher than 1.1 (1.31 ± 0.10) which is an important criterion to classify the $a\dot{V}O_{2-peak}$ as "maximum" aerobic power (43); however, there are still discussions on how to properly identify maximum $a\dot{V}O_2$ during incremental exercise (46). Therefore, the $a\dot{V}O_{2-peak}$ was used as an index related to maximal aerobic power.

2.4.1 Noise Analysis

One of the major issues related to the aerobic fitness evaluation based on $a\dot{V}O_2$ is the random noise associated with the metabolic carts and the intra-breath fluctuations that influence the confidence of the estimated indexes (27, 35). In addition, the signal steady-state amplitude also influences the quality of the parameter's estimation because it determines the proportion of the signal that is discernible from the noise, where a higher amplitude counterbalances the negative influences of random noise (40). As initially proposed by this study, it is essential to investigate the impact of the proportion between the signal amplitude and the noise level (or signal-to-noise ratio) over the aerobic fitness parameters estimation (17, 27, 35) since it can influence the investigation of the relationship between maximal aerobic power with aerobic fitness.

For the $a\dot{V}O_{2-max}$ calculation, the noise influences may be neglected most of the time because very high $a\dot{V}O_2$ amplitudes during the peak of the CPET decrease the noise contribution up to only ~3% (45) so the signal-to-noise ratio for a $a\dot{V}O_{2-peak}$ of, for example, ~2.5 $l \cdot min^{-1}$, is 0.031 $l \cdot min^{-1}$ (45). In addition, since $a\dot{V}O_{2-peak}$ estimation does not include any complex data transformation/modeling beyond a simple average, the degree of freedom of this estimate is much lower than the methods used to estimate the aerobic fitness (40) so the confidence of $a\dot{V}O_{2-max}$ estimation relies even less on the signal-to-noise ratio.

The study of the influences of the noise level and the amplitude over the parameters estimate was initially investigated by computer simulations (next section). The noise level of each participant was calculated as the SD (in $l \cdot min^{-1}$) of the $a\dot{V}O_2$ during the last two minutes of the CWR, and the steady state amplitude (also in $l \cdot min^{-1}$) was taken as the mean response of the last minute minus the mean $a\dot{V}O_2$ during the last minute of the CWR baseline. Finally, the signal-to-noise ratio was obtained by dividing the steady state amplitude by the noise level.

2.4.1.1 Computer Simulations

The algorithm used to build the computer simulations was previously described elsewhere (8, 9). The simulated $a\dot{V}O_2$ time series response to an CWR and PRBS protocol (with a work rate variation between 25 and 100 watts) were built from the combinatorial analysis of the following parameters range: $10 < \tau < 90$ s (increment of 1 s) and 150 < steady state amplitude < 1650 $ml \cdot min^{-1}$ (every 75 $ml \cdot min^{-1}$). Each of these simulations was distorted by a white noise generator with a magnitude varying from 0 (without noise, for reference) to 450 ml·min^{-1} (every 5ml·min^{-1}) resulting in 152,919 simulations with different aerobic system speeds, amplitudes and noise level, for each protocol (CWR and PRBS). The signal-to-noise of these simulations ranged from 0.3 to 330. Since τ, MNG, and CCF_{peak} are not influenced by baseline values, no baseline was added to the simulations. The τ range of these simulations was selected in order to include the same τ range of the experimental data (that was previously calculated).

Figure 6 describes some examples of the simulations with a constant τ of 25 s but varied noise and steady state amplitudes, resulting in signals with remarkably high (Figure 6 A) and very low (Figure 6 D) signal-to-noise ratio. Higher noise can be counterbalance with higher amplitude (Figure 6 B), and lower amplitude can be counterbalanced by lower noise (Figure 6 C), maintaining a more reliable signal-to-noise ratio.

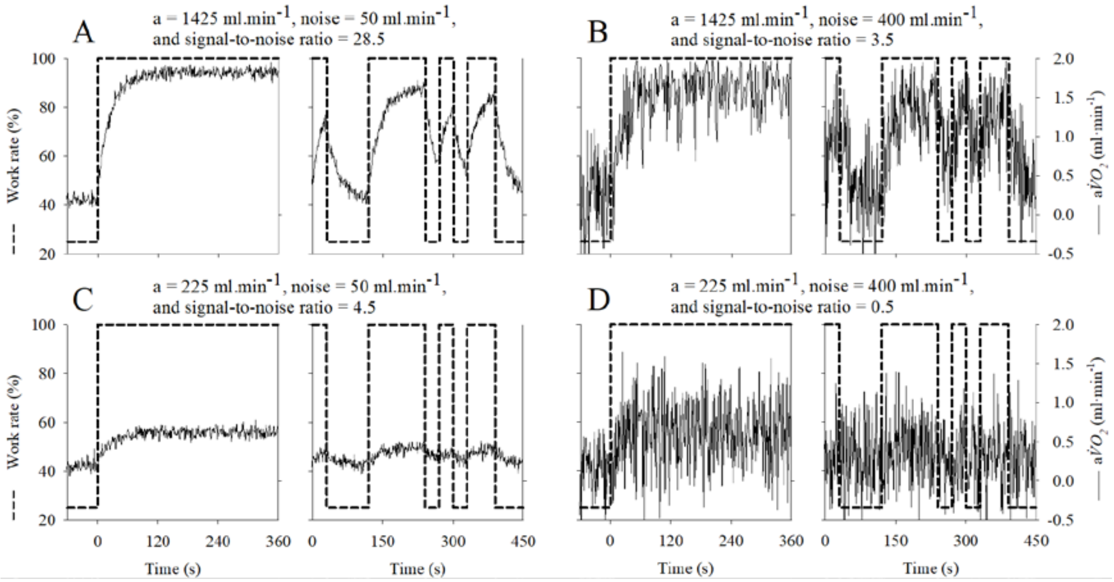

Figure 6. Computer simulations of the alveolar oxygen uptake ($a\dot{V}O_2$) response to a constant and pseudorandom binary sequence exercise protocols. The $a\dot{V}O_2$ responses have different steady state amplitudes (a = 225 and 1425 ml·min^{-1}) and noise levels (50 and 400 ml·min^{-1}) resulting in a signal-to-noise ratio of 28.5, 3.5, 4.5, and 0.5 in A, B, C, and D, respectively. Higher amplitudes associated with lower noise levels result in remarkably high signal-to-noise ratio (A), and the opposite, in very low signal-to-noise ratio (D). Higher noise can be counterbalance with higher amplitude (B), and lower amplitude can be counterbalanced by lower noise (C), maintaining a reliable signal-to-noise ratio.

The aerobic fitness parameters, τ (from CWR protocol), MNG and CCF_{peak} (both from PRBS protocol), were calculated as previously described in the text for each simulated data. However, for τ estimation, the cardio-dynamic phase was not removed from the CWR data because only the phase of interest was simulated (8). For each of the simulations, the error of the parameter estimate was taken as the difference, in percentage, between the estimated parameter with its analogous estimate from the zero-noise signal.

The computer program used to generate the simulations was designed as following. First, as previously described (8, 9), the software builds the second-by-second oxygen uptake response to a standard constant workload and pseudorandom binary sequence (PRBS) exercise protocol following an exponential function for both, on and off dynamic responses, using the function parameters (τ, and steady-state amplitude) inputted by the user. Second, the software generates the white noise time series from an embedded LabVIEW function (https://zone.ni.com/reference/en-XX/help/371361R-01/lvanls/gaussian_white_noise/) with the same length of the exercise protocols, and with an amplitude defined by the user. Third, the noise is added, second-by-second, to the simulated response to generate the distorted simulations. Finally, the indexes τ, MNG, and CCF_{peak} are estimated from the distorted responses. Figure 7 shows the distorted response for a constant workload (A) and PRBS (B) exercise protocols. The constant workload data fitting, when τ is estimated, is displayed in Figure 7 C, and the frequency analysis of the PRBS, to calculate the MNG, is displayed in Figure 7 D. The cross-correlation function of the response during the PRBS, and its peak, are demonstrated in E.

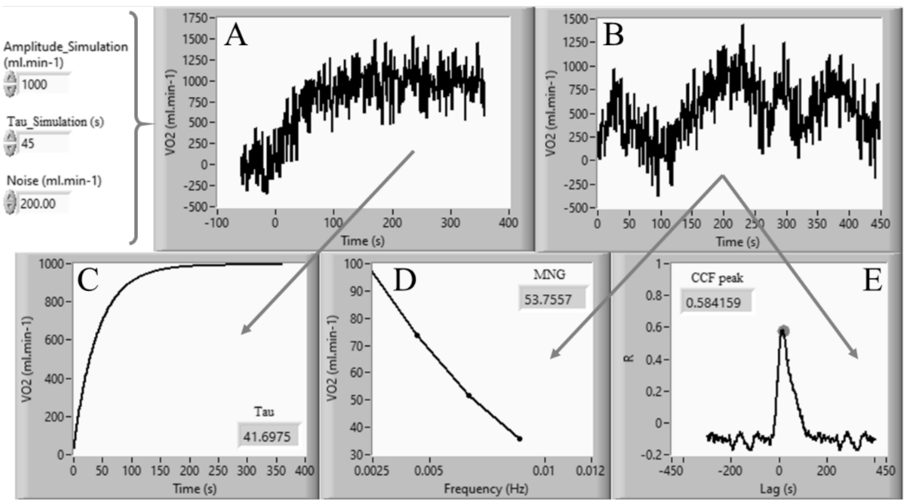

Figure 7. LabVIEW implementation of the computer program to generate the oxygen uptake simulations with different noise levels. This software has three inputs (amplitude, tau and noise) and three outputs (time constant tau [τ], mean normalized gain [MNG] and cross-correlation peak [CCF_{peak}]). Please see text for more details. The software block diagram can be download at: https://doi.org/10.6084/m9.figshare.12206663.v1 (Supplementary Material 2). Program built on NI LabVIEW Student Edition - 2014, personal and research use only.

3. Statistics

Most of the experimental data were normally distributed so the correlation level between $a\dot{V}O_{2-peak}$ with each of the aerobic fitness indexes (τ, MNG and CCF_{peak}) was calculated by Pearson's product moment correlation coefficient (R) (41). From R and sample size, the t statistic and degree of freedom were calculated and then used to obtain the two-tailed statistical significance level (p value). Despite the null-hypothesis significance testing is being currently deprecated (Ho et al., 2019; Wasserstein et al., 2019), the behavior of the p-values of the correlations across the different signal-to-noise levels will be visually analyzed.

Since the signal-to-noise ratio appears to influence the confidence of the aerobic fitness parameter estimates (27, 35), participants were firstly ranked according to the signal-to-noise ratio. Afterwards, the participant with the lowest signal-to-noise ratio was removed from the sample and the correlation coefficient between the variables was tested. This procedure was performed recursively from a sample size of 43 (all participants) to 3 (lowest possible sample size for the statistical testing). As expected, the signal-to-noise ratio progressively increased (from 5.8 ± 2.2 to 11.3 ± 1.0) as the participants with the lowest signal-to-noise ratio were removed from the sample (Figure 8) which allowed us to test the influences of the signal-to-noise ratio over the correlation of the studied parameters. However, while the signal-to-noise increases, the sample size decreases, and the probability of finding statistical differences, if present, also decreases. This statistical balance was investigated throughout this study by analyzing the R and p values simultaneously as a function of the mean signal-to-noise ratio.

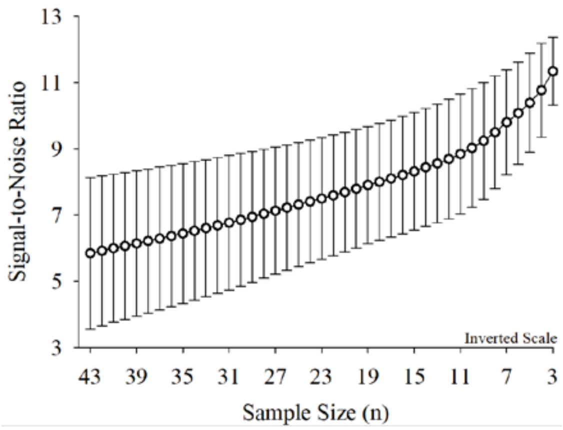

Figure 8. Relationship between mean ± SD signal-to-noise ratio and the study sample size. Participants were ranked according to their signal-to-noise ratio and then those with the lowest signal-to-noise were removed from the sample. As expected, the mean signal-to-noise increased as the sample size decreased.

Finally, the influence of the signal-to-noise ratio over the tested correlations was verified by the linear regression analysis (R^2 and p value) between the mean signal-to-noise ratio of the participants with the R from the correlation between maximal aerobic power ($a\dot{V}O_{2-peak}$) and each of the parameters for aerobic fitness evaluation (τ, MNG and CCF_{peak}). Linear regression analysis was also used to verify the influence of the signal-to-noise ratio over the correlation between the parameters used to evaluate the aerobic fitness level (τ, MNG, and CCF_{peak}).

4. Results

The computer simulations will be firstly described, followed by the correlation between the maximal aerobic power ($a\dot{V}O_{2-peak}$) with the aerobic fitness parameters (τ, MNG, and CCF_{peak}) as a function of the signal-to-noise ratio.

4.1 Noise Analysis of Computer Simulations

As displayed in Figure 9, the noise level and steady-state amplitude of the computer simulations are plotted as colored intensity graphs (error of estimation). The code used to generate these graphs is described in Supplementary Material 3 (https://doi.org/10.6084/m9.figshare.12196092.v1). For a better data visualization, only errors for the interval 0-90% were considered into these graphs (the complete dataset can be found in Supplementary Material 4 (https://doi.org/10.6084/m9.figshare.12018171). On top of the simulated data, the experimental data are plotted for reference. Some examples of signal-to-noise ratio are also plotted in Figure 9. For all parameters related to aerobic fitness (τ in A, MNG in B, and CCF_{peak} in C), the uncertainty of the parameter estimate (colors) increases as a function of the noise level and decreases as a function of the steady state amplitude. Between the graphs in Figure 6, the uncertainty of τ estimates (Figure 9 A) was higher than MNG (Figure 9 B) and CCF_{peak} (Figure 9 C) for the signal-to-noise range from 2 to 20 (participants range). Between MNG (Figure 9 B) and CCF_{peak} (Figure 9 C), most of participants are located at <0 to 15% interval of the expected estimate errors. For all simulations, except in 11 cases for CCF_{peak} estimation (only 0.0058% of the total simulations), all parameters were associated to a certain degree of uncertainty (error of estimation higher than zero), independently of the signal-to-noise ratio.

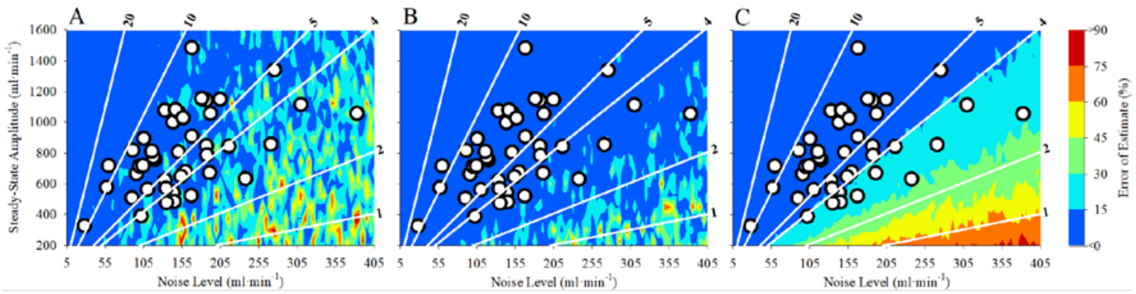

Figure 9. Computer simulations of the alveolar oxygen uptake response during exercise transitions with variable noise levels and steady state amplitudes. As displayed in A, B and C, the simulated data were analyzed by time domain modelling (by the time constant τ), frequency domain analysis (by the mean normalized gain, or MNG) and by the peak of the cross-correlation function (CCF_{peak}), respectively. For each of the simulations, the error of the parameter estimate (colors) was taken as the difference, in percentage, between the estimated parameter with its analogous estimate from the zero-noise signal. The noise level and the steady state amplitude of the experimental data from the constant work rate tests (participants data, open circle) were plotted within this reference frame. Some examples of the signal-to-noise ratio (i.e., steady-state amplitude/noise level) are also plotted as white solid lines. See text for further details about the computer simulations.

4.2 Relationship Between Aerobic Fitness and Power

The correlation between the maximal aerobic power with aerobic fitness was tested by the correlation coefficient R and its p value between the $a\dot{V}O_{2-peak}$ (maximal aerobic power level) with the aerobic fitness parameters (τ, MNG and CCF_{peak}) at different combinations of signal-to-noise ratio and sample sizes (Figure 10).

As described in Figure 10 A, the aerobic fitness evaluated by τ was correlated with maximal aerobic power (i.e., $a\dot{V}O_{2-peak}$) with a R of ~ - 0.5 on average across the tested signal-to-noise ratio values and sample sizes. As verified by the linear regression, the correlation coefficient between τ and $a\dot{V}O_{2-peak}$ was influenced (R= -0.92) by the signal-to-noise ratio and decreased (towards -1) 0.109 per unit of signal-to-noise ratio.

As demonstrated in Figure 10 B, the aerobic fitness evaluated by the MNG was correlated with maximal aerobic power (i.e., $a\dot{V}O_{2-peak}$) with a R ~ - 0.4 on average across the tested mean signal-to-noise ratios. As verified by the linear regression, the correlation coefficient between MNG and $a\dot{V}O_{2-peak}$ was also influenced (R= 0.80) by the signal-to-noise ratio and increased 0.078 per unit of signal-to-noise ratio.

The aerobic fitness evaluated by the CCF_{peak} (Figure 10 C) was correlated with maximal aerobic power (i.e., $a\dot{V}O_{2-peak}$) with a R ~ 0.4 in average. However, as verified by the linear regression, the correlation coefficient between CCF_{peak} with $a\dot{V}O_{2-peak}$ was not influenced by the signal-to-noise ratio. The sample size of the linear correlation only has 41 datapoints because the correlations were only calculated with a minimum sample size of 3 participants.

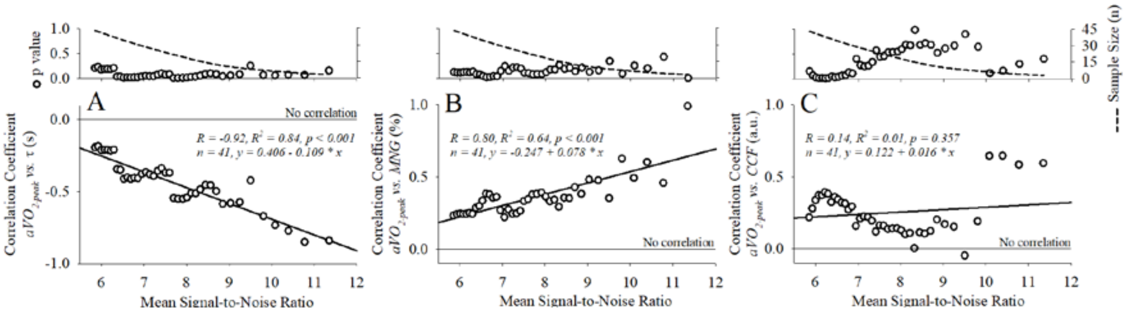

Figure 10. Correlations between the measured aerobic fitness parameters (tau [τ], in A; mean normalized gain [MNG], in B; and cross-correlation function peak [CCF_{peak}], in C) with maximal aerobic power evaluated by peak alveolar oxygen uptake ($a\dot{V}O_{2-peak}$) at different signal-to-noise ratios estimated from the constant work rate tests (x axis in A, B and C). The correlation coefficient is plotted in the lower A, B and C graphs, and the statistical significance level (p value, open circles) and the sample size (dotted lines) are displayed in the upper graphs as a function of the signal-to-noise ratio. A regression analysis between the correlation coefficients and the signal-to-noise ratio was also performed.

5. *Discussion*

Our results confirmed our initial hypothesis that a slower aerobic system response during exercise transitions (aerobic fitness) is associated with lower maximal aerobic power. This association was dependent on the signal-to-noise ratio and the method used to evaluate aerobic fitness. For the first time, these results demonstrate that the correlation between maximal aerobic power and aerobic fitness was dependent on the degree of uncertainty of the aerobic fitness parameter estimates that are directly related to the $a\dot{V}O_2$ signal-to-noise ratio.

5.1 *Noise Analysis*

The expected influences of the signal-to-noise ratio, as the proportion between the steady-state amplitude and the noise level, on the parameter estimates were initially investigated by computer simulations. The behavior of the error of τ estimates, as a function of noise level and steady-state amplitude (Figure 9 A), was less homogeneous probably due to the additional degree of uncertainty from the Levenberg–Marquardt algorithm used in time-domain explicit data fitting (40). Likewise, the error of estimate for the MNG and CCF_{peak} (Figures 9 B and 9 C, respectively) increased with higher noise and smaller steady-state amplitude. The counter balancing effect of a higher steady-state amplitude over a higher noise can be seen for all parameters. In practical terms, Figure 9 can be used to estimate the expected uncertainty the aerobic fitness parameter estimates for a given known steady-state amplitude and noise level.

The comparison between the experimental data and the computer simulations allowed us to identify that there was some level of expected uncertainty of the aerobic fitness evaluation in the participants included into this study, which appeared to compromise the correlation between maximal aerobic power and aerobic fitness. If the aerobic fitness is correlated with maximal aerobic power, this expected error should be further investigated to avoid type I error due to the probability of including fitness indexes with high estimation uncertainty. When each participant's noise and steady-state amplitude were plotted on the top of the simulated data, it was possible to see that most of participants were at the desired <0 to 15% error interval when the aerobic fitness was evaluated by MNG and CCF_{peak} (Figures 9 B and 9 C, respectively). On the other hand, when aerobic fitness was evaluated by τ (Figure 9 A), the expected uncertainty was higher than MNG and CCF_{peak}, showing that, at least for the tested participants, τ estimation may rely more on signal-to-noise ratio to decrease estimation uncertainty, which is in accordance to previous literature (27).

Since $\dot{W}$ changes in CWR and PRBS protocols were related to 20 and 80% of the GET, participants were already close to the moderate-to-intense domain transition which means that the steady-state amplitude was as high as possible and close to the upper ceiling of the moderate intensity domain. When the GET is not available, the choice of selecting higher $\dot{W}$ to increase the signal-to-noise ratio may decrease the error of estimates, however; it might also introduce non-linearities if the exercise domain switches to intense (20, 24).

Using the reference lines in Figure 9, a signal-to-noise ratio lower than ~10, ~2 and ~4 was associated to a maximum error of only 15% when the aerobic fitness was evaluated by τ, MNG and CCF_{peak} (Figures 9 A, 9 B and 9 C, respectively). The intrinsic low-pass filtering characteristics of MNG calculations (7–9) may explain the smaller uncertainty of its estimation in comparison with τ and CCF_{peak}. Since CCF_{peak} calculation does not involve any estimation beyond a peak identification of the second-by-second correlation between the shifted $a\dot{V}O_2$ time series across the PRBS exercise protocol (31), the uncertainty is linearly defined by the signal-to-noise ratio (as demonstrated by Figure 9 C).

The computer simulations allowed us to speculate that: 1-) for all indexes used for aerobic fitness level evaluation, there was always a certain expected degree of uncertainty, independently of the signal-to-noise ratio, and 2-) the uncertainty level of τ estimation was higher than the uncertainty of MNG and CCF_{peak} estimation.

5.2 Relationship Between Aerobic Fitness and Power

In 2016, a study (55) elucidated a model that can be used to explain, at least partially, the expected relationship between maximal aerobic power and fitness (7, 54) where a slower aerobic response to a new metabolic demand might be related to a lower maximal aerobic power by limiting the functional capacity. During incremental exercise protocols used to measure $a\dot{V}O_{2-peak}$ (maximal aerobic power), the expected linear relationship between work rate ($\dot{W}$) and $a\dot{V}O_2$ seems to be explained by a progressive, and balanced, slower aerobic response and higher system gain (i.e., $a\dot{V}O_2/\dot{W}$ ratio) (55). Despite the literature debate on the relationship between aerobic system gain and muscle fatigue (25), the progressive loss of muscle homeostasis and efficiency during incremental exercise seems to be related to the progressive increase in type II fibers recruitment that has less oxidative capacity per unit of $\dot{W}$ (i.e., higher gain) (3, 30). Accordingly, during incremental exercise, a slower aerobic system response to each work rate step increase is followed by a higher system gain (maintaining the linearity between $a\dot{V}O_2$ and $\dot{W}$), which should lead to a lower exercise capacity, thus lower $a\dot{V}O_{2-peak}$. In fact, aerobic fitness, which is associated with effort perception, seems to be more related with exercise capacity than with the aerobic system gain by itself (15). Therefore, slower $a\dot{V}O_2$ response characterized by slower τ, and lower MNG and CCF_{peak} values, during moderate exercise protocols, should be associated with a lower exercise tolerance by the progressive accumulation of fatigue-related metabolites during the incremental protocols (26). It is plausible to predict that a "buildup" of slower dynamics throughout the incremental exercise would lead to a lower exercise capacity since higher anaerobic energy supply perturbances are related to time of exhaustion during very-intense exhaustive exercise (37). Therefore, the aerobic fitness might be one of, if not the greatest, determinants of the exercise capacity that is strictly related to maximal aerobic power.

As illustrated in Figure 10, maximal aerobic power was correlated with aerobic fitness (evaluated by τ, MNG and CCF_{peak}) for some specific combinations of signal-to-noise ratio and sample size. The effect of the signal-to-noise ratio on the correlation between $a\dot{V}O_{2-peak}$ with aerobic fitness was clearer when τ was used to estimate the fitness level (Figure 10 A). The correlation between $a\dot{V}O_{2-peak}$ and τ increased as the mean signal-to-ratio increased, as demonstrated by the linear regression. The correlation between MNG with $a\dot{V}O_{2-peak}$ (Figure 10 B) was also influenced by the mean signal-to-noise level although to a lesser extent than τ, as demonstrated by the linear regression between the correlation level and the mean signal-to-noise ratio. These findings are supported by the initial computer simulations presented in Figure 9, where a higher signal-to-noise ratio decreased the uncertainty of the aerobic fitness parameter estimates which in turn increased the expected correlation level between $a\dot{V}O_{2-peak}$ with τ and MNG. The inherent filter of MNG calculation possibly decreased the dependence of the $a\dot{V}O_{2-peak}$ and MNG correlation from the signal-to-noise ratio.

On the other hand, in contrast with our initial hypothesis, the correlation between maximal aerobic power with CCF_{peak} (Figure 10 C) was not influenced by the signal-to-noise ratio but vastly influenced by the sample size where the p-values largely increased when the sample size was lower than ~ 35 participants. The higher dependency of CCF_{peak} on sample size might be related to the sensitivity of this parameter in evaluating the speed of the $a\dot{V}O_2$. In contrast to MNG which is optimized to evaluate the $a\dot{V}O_2$ speed of a physiological τ range from 10 to 100 s (9), the magnitude of CCF_{peak} changes decrease drastically when τ is higher than ~50 s (please check Figure 2 from (19)), which was the case in 16 (37%) participants. Therefore, since the correlation between CCF_{peak} and τ is not linear and tends to a constant level after τ slower than ~50 s, the aerobic fitness level evaluation by CCF_{peak} was compromised, thus higher sample sizes would compensate this lower sensitivity for slower responses.

A few more factors must be considered when comparing τ, MNG and CCF_{peak} with $a\dot{V}O_{2-peak}$ from the experimental data. First, in order to compare methods that are mostly used (8, 23, 31) for aerobic fitness evaluation during PRBS protocols, the MNG and CCF_{peak} were calculated from two complete 450 s exercise sequences. Thus, in contrast to τ that was estimated based on a single transition (8), the dataset used for MNG and CCF_{peak} calculations may have had a higher signal-to-noise ratio, despite a previous study demonstrating no major differences in τ estimation based on simulated data from different combinations of exercise repetitions (17). Commonly, τ is estimated from the ensemble-averaged $a\dot{V}O_2$ data from multiple exercise repetitions performed at different days or within the same laboratory visit, which should improve the signal-to-noise and the expected correlation between τ and $a\dot{V}O_{2-peak}$. However, one of the purposes of this study was to test the methods that could in fact be used in a single visit (like the $a\dot{V}O_{2-peak}$) to evaluate aerobic fitness from τ (12), MNG (9) and CCF_{peak} (19, 32).

Second, since we are comparing the aerobic fitness indexes with $a\dot{V}O_{2-peak}$, we must also consider that the $a\dot{V}O_{2-peak}$ by itself might be also a source of error that may influence the correlations presented in this study. However, $a\dot{V}O_{2-peak}$ calculation, in contrast to the aerobic fitness indexes obtained during the moderate intensity exercise protocols, only requires a simple averaging of the last 20 seconds of data. In addition, the signal-to-noise ratio at the $a\dot{V}O_{2-peak}$ is vastly higher than the $a\dot{V}O_2$ during the CWR and PRBS protocols due to the nature of the incremental exercise where the peak value is more discernible from the random noise around the mean. During the peak of incremental exercise, considering an expected error level of 0.15 l·min^{-1} and a $a\dot{V}O_{2-peak}$ of 2.94 l·min^{-1} (group mean response), the signal-to-noise-ratio of 19 indicates that the noise might be negligible. On the other hand, this same 0.15 l·min^{-1} of noise is expected to impact the aerobic fitness parameter estimates if the steady-state amplitude is not large enough to compensate this noise.

It is important to point out that the participants were recursively removed from the sample not to improve the correlations but to increase, progressively, the signal-to-noise ratio which turned out improved the correlation between power and fitness when aerobic fitness was evaluated by τ and MNG (Figure 10). This study design shows that the correlation between maximal aerobic power and aerobic fitness was modified by the quality of the $a\dot{V}O_2$ data that influences uncertainty of the parameter estimates, at least when aerobic fitness was evaluated by τ and MNG. For CCF_{peak}, the speed of the $a\dot{V}O_2$ seemed to also influence its correlation with $a\dot{V}O_{2-peak}$.

Aerobic fitness level evaluation has some advantages over maximal aerobic power assessment as, beyond others, it can be evaluated during moderate intensity exercise. Thus, aerobic fitness can be more broadly investigated in sedentary or less healthy individuals (26, 38) who are not able to push themselves to the peak volitional fatigue. When compared to maximal incremental protocols used to measure $a\dot{V}O_{2-peak}$, moderate intensity exercise testing has lower risks than those associated with maximal exertion (48) and can be monitored outside of the laboratory confinements (5). However, $a\dot{V}O_{2-peak}$ is still the most common tool to evaluate CRH (34, 47) and does not require any complex data analysis beyond a simple data averaging at the peak of the exercise which is an advantage over aerobic fitness evaluation methods because it is less susceptible to random noise.

The challenges of applying maximum exercise testing in patients with chronic diseases for example make aerobic fitness investigation by indexes such as τ, MNG, or CCF_{peak} a strong candidate for CRH evaluation if an acceptable signal-to-noise ratio is reached. Our results showed that, at least to some extent, moderate exercise protocols might be as good as maximum exertion exercise protocols to obtain indexes related to CRH. As practical recommendations, we suggest the use of PRBS or multiple repetitions of CWR protocol to evaluate aerobic fitness when a proper signal-to-noise ratio is reached. If the steady-state amplitude and baseline noise are known, Figure 9 can be used to estimate the expected uncertainty of the aerobic fitness indexes.

6 *Study Limitations*

This study has some limitations that must be considered. No patients were included into the sample, and the maximum aerobic power range was relatively small (from 1.49 to 4.55 l·min^{-1}), thus more studies are necessary to expand these findings to populations with chronic diseases for example. In addition, since we are evaluating the influences of random noise around the mean expected $a\dot{V}O_2$ response, it was assumed a constant noise across the entire simulated and experimental data, so the noise was not dependent on the tested work rates. However, we may also consider that different noise levels might be present at different work rates within the same participant.

7. *Conclusion*

Aerobic fitness is related to maximum aerobic power in healthy subjects; however, this association appeared to be dependent on the signal-to-noise ratio and the data analysis method used for aerobic fitness evaluation. Our results suggest that sub-maximal exercise protocols (such as CWR and PRBS) might be as good as maximum exertion exercise protocols to obtain indexes related to cardiorespiratory health; however, extra caution is necessary for the methods used to evaluate aerobic fitness due to their high dependency on signal-to-noise ratio.

8. *Conflict of interest*

The authors declare no conflict of interest.

9. *References*

1. **Alexander NB**, **Dengel DR**, **Olson RJ**, **Krajewski KM**. Oxygen-uptake (VO2) kinetics and functional mobility performance in impaired older adults. *J Gerontol A Biol Sci Med Sci* 58: 734–739, 2003.

2. **Barstow TJ**, **Buchthal S**, **Zanconato S**, **Cooper DM**. Muscle energetics and pulmonary oxygen uptake kinetics during moderate exercise. *J Appl Physiol* 77: 1742–1749, 1994.

3. **Barstow TJ**, **Jones AM**, **Nguyen PH**, **Casaburi R**. Influence of muscle fiber type and pedal frequency on oxygen uptake kinetics of heavy exercise. *J Appl Physiol* 81: 1642–1650, 1996.

4. **Beaver WL**, **Wasserman K**, **Whipp BJ**. A new method for detecting anaerobic threshold by gas

exchange. *J Appl Physiol* 60: 2020–2027, 1986.

5. **Beltrame T**, **Amelard R**, **Wong A**, **Hughson RL**. Extracting aerobic system dynamics during unsupervised activities of daily living using wearable sensor machine learning models. *J. Appl. Physiol.* (June 8, 2017). doi: 10.1152/japplphysiol.00299.2017.
6. **Beltrame T**, **Hughson RL**. Aerobic system analysis based on oxygen uptake and hip acceleration during random over-ground walking activities. *Am J Physiol - Regul Integr Comp Physiol* 312, 2017.
7. **Beltrame T**, **Hughson RL**. Aerobic system analysis based on oxygen uptake and hip acceleration during random over-ground walking activities. *Am J Physiol - Regul Integr Comp Physiol* 312: R93–R100, 2017.
8. **Beltrame T**, **Hughson RL**. Linear and non-linear contributions to oxygen transport and utilization during moderate random exercise in humans. *Exp Physiol* 102: 563–577, 2017.
9. **Beltrame T**, **Hughson RL**. Mean Normalized Gain: A New Method for the Assessment of the Aerobic System Temporal Dynamics during Randomly Varying Exercise in Humans. *Front Physiol* 8, 2017.
10. **Beltrame T**, **Rodrigo V**, **Hughson RL**. Sex differences in the oxygen delivery, extraction, and uptake during moderate-walking exercise transition. *Appl Physiol Nutr Metab* 42, 2017.
11. **Beltrame T**, **Villar R**, **Hughson RL**. Sex differences in the oxygen delivery, extraction, and uptake during moderate-walking exercise transition. *Appl. Physiol. Nutr. Metab.* (June 2017). doi: 10.1139/apnm-2017-0097.
12. **Borghi-Silva A**, **Beltrame T**, **Reis MS**, **Sampaio LMM**, **Catai AM**, **Arena R**, **Costa D**. Relationship between oxygen consumption kinetics and BODE index in COPD patients. *Int J COPD* 7, 2012.
13. **Despres J-P**. Physical Activity, Sedentary Behaviours, and Cardiovascular Health: When Will Cardiorespiratory Fitness Become a Vital Sign? *Can J Cardiol* 32: 505–513, 2016.
14. **Drescher U**, **Schmale R**, **Koschate J**, **Thieschafer L**, **Schiffer T**, **Schneider S**, **Hoffmann U**. Non-invasive estimation of muscle oxygen uptake kinetics with pseudorandom binary sequence and step exercise responses. *Eur J Appl Physiol* 118: 429–438, 2018.
15. **Duffield R**, **Edge J**, **Bishop D**, **Goodman C**. The relationship between the over(V,˙) O2 slow component, muscle metabolites and performance during very-heavy exhaustive exercise. *J. Sci.*

Med. Sport (2007). doi: 10.1016/j.jsams.2006.05.013.

16. **Eßfeld D**, **Hoffmann U**, **Stegemann J**. A model for studying the distortion of muscle oxygen uptake patterns by circulation parameters. *Eur J Appl Physiol Occup Physiol* 62: 83–90, 1991.

17. **Francescato MP**, **Cettolo V**, **Bellio R**. Confidence intervals for the parameters estimated from simulated O2 uptake kinetics: effects of different data treatments. *Exp Physiol* 99: 187–195, 2014.

18. **Hill A V**, **Lupton H**. Muscular Exercise, Lactic Acid, and the Supply and Utilization of Oxygen. *QJM An Int J Med* os-16: 135–171, 1923.

19. **Hoffmann U**, **Drescher U**, **Benson AP**, **Rossiter HB**, **Essfeld D**. Skeletal muscle $\dot{V}O_2$ kinetics from cardio-pulmonary measurements: Assessing distortions through O2 transport by means of stochastic work-rate signals and circulatory modelling. *Eur J Appl Physiol* 113: 1745–1754, 2013.

20. **Hoffmann U**, **Eßfeld D**, **Leyk D**, **Wunderlich HG**, **Stegemann J**. Prediction of individual oxygen uptake on-step transients from frequency responses. *Eur J Appl Physiol Occup Physiol* 69: 93–97, 1994.

21. **Hoffmann U**, **Eßfeld D**, **Wunderlich HG**, **Stegemann J**. Dynamic linearity of VO2 responses during aerobic exercise. *Eur J Appl Physiol Occup Physiol* 64: 139–144, 1992.

22. **Howley ET**, **Bassett DR**, **Welch HG**. Criteria for maximal oxygen uptake: review and commentary. *Med. Sci. Sports Exerc.* 27: 1292–1301, 1995.

23. **Hughson RL**, **Winter DA**, **Patla AE**, **Swanson GD**, **Cuervo LA**. Investigation of VO2 kinetics in humans with pseudorandom binary sequence work rate change. *J Appl Physiol* 68: 796–801, 1990.

24. **Hughson RL**, **Xing HC**, **Borkhoff C**, **Butler GC**. Kinetics of ventilation and gas exchange during supine and upright cycle exercise. *Eur J Appl Physiol Occup Physiol* 63: 300–307, 1991.

25. **Jones AM**, **Grassi B**, **Christensen PM**, **Krustrup P**, **Bangsbo J**, **Poole DC**. Slow component of $\dot{V}o_2$ kinetics: Mechanistic bases and practical applications. *Med. Sci. Sports Exerc.* (2011). doi: 10.1249/MSS.0b013e31821fcfc1.

26. **Jones AM**, **Poole DC**. Oxygen Uptake Kinetics in Sport, Exercise and Medicine [Online]. Routledge. http://books.google.ca/books/about/Oxygen_Uptake_Kinetics_in_Sport_Exercise.html?id=nEdiW1N0syIC&pgis=1.

27. **Keir DA**, **Murias JM**, **Paterson DH**, **Kowalchuk JM**. Breath-by-breath pulmonary O2 uptake

kinetics: effect of data processing on confidence in estimating model parameters. *Exp Physiol* 99: 1511–22, 2014.

28. **Keir DA**, **Robertson TC**, **Benson AP**, **Rossiter HB**, **Kowalchuk JM**. The influence of metabolic and circulatory heterogeneity on the expression of pulmonary VO2 kinetics in humans. *Exp Physiol* 101: 176–192, 2016.

29. **Kerlin TW**. Properties of Important Test Signals. In: *Frequency Response Testing in Nuclear Reactors*. Elsevier, 1974, p. 52–82.

30. **Koppo K**, **Bouckaert J**, **Jones AM**. Effects of Training Status and Exercise Intensity on Phase II V̇O 2 Kinetics. *Med. Sci. Sports Exerc.* (2004). doi: 10.1249/01.MSS.0000113473.48220.20.

31. **Koschate J**, **Drescher U**, **Thieschafer L**, **Heine O**, **Baum K**, **Hoffmann U**. Cardiorespiratory Kinetics Determined by Pseudo-Random Binary Sequences - Comparisons between Walking and Cycling. *Int J Sports Med* 37: 1110–1116, 2016.

32. **Koschate J**, **Drescher U**, **Thieschäfer L**, **Heine O**, **Baum K**, **Hoffmann U**. Cardiorespiratory Kinetics Determined by Pseudo-Random Binary Sequences – Comparisons between Walking and Cycling. *Int J Sport Med* 37: 1110–1116, 2016.

33. **Koschate J**, **Gerlich L**, **Wirtz V**, **Thieschäfer L**, **Drescher U**, **Hoffmann U**. Cardiorespiratory kinetics: comparisons between athletes with different training habits. *Eur. J. Appl. Physiol.* .

34. **Kunutsor SK**, **Laukkanen T**, **Laukkanen JA**. Cardiorespiratory Fitness is Associated with Reduced Risk of Respiratory Diseases in Middle-Aged Caucasian Men: A Long-Term Prospective Cohort Study. *Lung* 195: 607–611, 2017.

35. **Lamarra N**, **Whipp BJ**, **Ward SA**, **Wasserman K**. Effect of interbreath fluctuations on characterizing exercise gas exchange kinetics. *J Appl Physiol* 62: 2003–2012, 1987.

36. **Lee D**, **Artero EG**, **Sui X**, **Blair SN**. Mortality trends in the general population: the importance of cardiorespiratory fitness. *J Psychopharmacol* 24: 27–35, 2010.

37. **Linnarsson D**, **Karlsson J**, **Fagraeus L**, **Saltin B**. Muscle metabolites and oxygen deficit with exercise in hypoxia and hyperoxia. *J. Appl. Physiol.* (1974). doi: 10.1152/jappl.1974.36.4.399.

38. **Manns PJ**, **Tomczak CR**, **Jelani A**, **Haennel RG**. Oxygen uptake kinetics: Associations with ambulatory activity and physical functional performance in stroke survivors. *J. Rehabil. Med.* (2010). doi: 10.2340/16501977-0498.

39. **Megari K**. Quality of life in chronic disease patients. *Heal. Psychol. Res.* (2013). doi:

10.4081/hpr.2013.e27.

40. **Motulsky HJ**, **Ransnas LA**. Fitting curves to data using nonlinear regression: a practical and nonmathematical review. *FASEB J* 1: 365–374, 1987.

41. **Mukaka MM**. Statistics corner: A guide to appropriate use of correlation coefficient in medical research. *Malawi Med J* 24: 69–71, 2012.

42. **Murias JM**, **Spencer MD**, **Kowalchuk JM**, **Paterson DH**. Influence of phase I duration on phase II VO2 kinetics parameter estimates in older and young adults. *Am J Physiol - Regul Integr Comp Physiol* 301: 218–224, 2011.

43. **Nelson MD**, **Petersen SR**, **Dlin RA**. Effects of age and counseling on the cardiorespiratory response to graded exercise. *Med. Sci. Sports Exerc.* (2010). doi: 10.1249/MSS.0b013e3181b0e534.

44. **Peterka RJ**. Sensorimotor Integration in Human Postural Control. *J Neurophysiol* 88: 1097–1118, 2002.

45. **Poole DC**, **Jones AM**. Measurement of the maximum oxygen uptake $\dot{V}o_{2max}$: $\dot{V}o_{2peak}$ is no longer acceptable. *J Appl Physiol* 122: 997–1002, 2017.

46. **Poole DC**, **Jones AM**. Measurement of the maximum oxygen uptake V̇o2max: V̇o2peak is no longer acceptable [Online]. *J Appl Physiol* 122: 997 LP – 1002, 2017. http://jap.physiology.org/content/122/4/997.abstract.

47. **Ramírez-Vélez R**, **Correa-Bautista JE**, **Ramos-Sepúlveda JA**, **Piñeros-Álvarez CA**, **Giraldo LI**, **Izquierdo M**, **García-Hermoso A**, **Rodríguez-Rodríguez F**, **Cristi-Montero C**. Aerobic capacity and future cardiovascular risk in Indian community from a low-income area in Cauca, Colombia. *Ital J Pediatr* 43, 2017.

48. **Rochmis P**, **Blackburn H**. Exercise Tests: A Survey of Procedures, Safety, and Litigation Experience in Approximately 170,000 Tests. *JAMA J. Am. Med. Assoc.* (1971). doi: 10.1001/jama.217.8.1061.

49. **Ross RM**. ATS/ACCP statement on cardiopulmonary exercise testing. *Am J Respir Crit Care Med* 167: 1451–1451, 2003.

50. **Stone NM**, **Kilding AE**. Aerobic Conditioning for Team Sport Athletes. *Sport. Med.* 39: 615–642, 2009.

51. **Sui X**, **LaMonte MJ**, **Laditka JN**, **Hardin JW**, **Chase N**, **Hooker SP**, **Blair SN**. Cardiorespiratory

fitness and adiposity as mortality predictors in older adults. *JAMA* 298: 2507–2516, 2007.

52. **Wasserman K**, **Hansen J**, **Sue D**, **Stringer W**, **Whipp B**. *Principles of exercise testing and interpretation*. Philadelphia: 1999.

53. **Whipp BJ**, **Mahler M**, **West JB**. Pulmonary Gas Exchange, Organism and Environment. .

54. **Whipp BJ**, **Ward SA**. Pulmonary gas exchange dynamics and the tolerance to muscular exercise: effects of fitness and training. *Ann Physiol Anthropol* 11: 207–214, 1992.

55. **Wilcox SL**, **Broxterman RM**, **Barstow TJ**. Constructing quasi-linear $\dot{V}$O2 responses from nonlinear parameters. *J Appl Physiol* 120: 121–129, 2016.

56. **World Health Organization**. World Health Statistics 2017. *Geneva World Heal. Organ.* (2017). doi: ISBN 978-92-4-156548-6.

57. **World Health Organization**. Noncommunicable diseases [Online]. Homepage, 2019. https://www.who.int/en/news-room/fact-sheets/detail/noncommunicable-diseases [8 Aug. 2019].

58. **Xing HC**, **Cochrane JE**, **Yamamoto Y**, **Hughson RL**. Frequency domain analysis of ventilation and gas exchange kinetics in hypoxic exercise. [Online]. *J Appl Physiol* 71: 2394–2401, 1991. http://www.ncbi.nlm.nih.gov/pubmed/1778938.

Figures Legend

Figure 1. Digital shift register composed by 4 stages to generate pseudorandom binary sequence exercise protocols. The addition feedback module (∑) add the values of the first and the fourth stage and check the criteria statement. This result (0 or 1) is recorded and then inserted into stage 1, and the register is shifted to the right. The output sequence composed by 1 and 0 is transformed in the target work rates where 1 = 80 % and 0 = 20% of the gas exchange threshold.

Figure 2. LabVIEW implementation of the digital shift register described in Figure 1 to generate pseudorandom binary sequence (PRBS) exercise protocols. The software has 5 inputs: the number of digits, the unit length, the initial register seeds, and the two work rate levels. From these inputs, the shift register is populated, and the time series of protocol is built. The frequency analysis is also performed to evaluate the signal on frequency space. The inputs are controlled by the user through the program graphical interface and the outputs are also displayed. The exercise protocol on time domain can be exported from the "PRBS vs Time" graph. The software block diagram can be download at: https://doi.org/10.6084/m9.figshare.12206654 (Supplementary Material 1). This software was built on National Instruments LabVIEW Student Edition, 2014, for personal and scientific use only.

Figure 3. Illustration of the exercise protocols composed of a constant work rate (CWR), a pseudorandom binary sequence (PRBS), and a maximal cardiopulmonary exercise testing (CPET). The two work rates (36 and 144 watts) of the CWR and PRBS protocols corresponded to 20 and 80% of the work rate at the gas exchange threshold (GET) previously identified. The increment rate of the CPET protocol (16 watts.min^{-1} in this case) was calculated accordingly to participant's sex, weight, height, and age. The alveolar oxygen uptake ($a\dot{V}O_2$, in l·min^{-1}) response to these protocols is also plotted.

Figure 4. Illustration of the aerobic fitness evaluated by time domain analysis of the alveolar oxygen uptake ($a\dot{V}O_2$) dynamics during exercise transition. The $a\dot{V}O_2$ response to a step exercise protocol (A) is fitted into a delayed mono-exponential model (solid line in B) and the cardiodynamic phase (11 s, fine pattern area in C) is removed from the data by the analysis of the residuals (upper graphs). The remaining $a\dot{V}O_2$

data (C) are fitted into the same exponential model and the time constant τ of this function is obtained. Please see text for more information about data fitting.

Figure 5. Illustration of the aerobic fitness evaluation based on the analysis of the alveolar oxygen uptake ($a\dot{V}O_2$, solid lines) dynamics during a pseudorandom binary sequence exercise protocol (dashed lines). The second-by-second linearly interpolated data (A) of the two consecutives protocols were ensemble averaged to obtain a single response (B). The exercise protocol and the $a\dot{V}O_2$ were transformed into the frequency space by a fast Fourier transformation and the system gain was calculated by dividing the $a\dot{V}O_2$ by the protocol amplitude at each of the analyzed frequencies and then normalized by the gain at frequency 2.2 mHz. The average of the normalized gains (in %) of the frequencies 4.4, 6.6 and 8.8 mHz (C) was taken as the final index related to aerobic fitness (named Mean Normalized Gain, or MNG). In addition, the exercise protocol work rate (upper graph in B) was cross-correlated with the $a\dot{V}O_2$ response (lower graph in B) accordingly to previous study (19) to obtain the cross-correlation function at different lags. The peak of CCF (CCF_{peak} in D) is also related to the speed of the $a\dot{V}O_2$ dynamics, as the MNG.

Figure 6. Computer simulations of the alveolar oxygen uptake ($a\dot{V}O_2$) response to a constant and pseudorandom binary sequence exercise protocols. The $a\dot{V}O_2$ responses have different steady state amplitudes (a = 225 and 1425 ml·min^{-1}) and noise levels (50 and 400 ml·min^{-1}) resulting in a signal-to-noise ratio of 28.5, 3.5, 4.5, and 0.5 in A, B, C, and D, respectively. Higher amplitudes associated with lower noise levels result in remarkably high signal-to-noise ratio (A), and the opposite, in very low signal-to-noise ratio (D). Higher noise can be counterbalance with higher amplitude (B), and lower amplitude can be counterbalanced by lower noise (C), maintaining a reliable signal-to-noise ratio.

Figure 7. LabVIEW implementation of the computer program to generate the oxygen uptake simulations with different noise levels. This software has three inputs (amplitude, tau and noise) and three outputs (time constant tau [τ], mean normalized gain [MNG] and cross-correlation peak [CCF_{peak}]). Please see text for more details. The software block diagram can be download at: https://doi.org/10.6084/m9.figshare.12206663.v1 (Supplementary Material 2). Program built on NI LabVIEW Student Edition - 2014, personal and research use only.

Figure 8. Relationship between mean ± SD signal-to-noise ratio and the study sample size. Participants were ranked according to their signal-to-noise ratio and then those with the lowest signal-to-noise were removed from the sample. As expected, the mean signal-to-noise increased as the sample size decreased.

Figure 9. Computer simulations of the alveolar oxygen uptake response during exercise transitions with variable noise levels and steady state amplitudes. As displayed in A, B and C, the simulated data were analyzed by time domain modelling (by the time constant τ), frequency domain analysis (by the mean normalized gain, or MNG) and by the peak of the cross-correlation function (CCF_{peak}), respectively. For each of the simulations, the error of the parameter estimate (colors) was taken as the difference, in percentage, between the estimated parameter with its analogous estimate from the zero-noise signal. The noise level and the steady state amplitude of the experimental data from the constant work rate tests (participants data, open circle) were plotted within this reference frame. Some examples of the signal-to-noise ratio (i.e., steady-state amplitude/noise level) are also plotted as white solid lines. See text for further details about the computer simulations.

Figure 10. Correlations between the measured aerobic fitness parameters (tau [τ], in A; mean normalized gain [MNG], in B; and cross-correlation function peak [CCF_{peak}], in C) with maximal aerobic power evaluated by peak alveolar oxygen uptake ($a\dot{V}O_{2-peak}$) at different signal-to-noise ratios estimated from the constant work rate tests (x axis in A, B and C). The correlation coefficient is plotted in the lower A, B and C graphs, and the statistical significance level (p value, open circles) and the sample size (dotted lines) are displayed in the upper graphs as a function of the signal-to-noise ratio. A regression analysis between the correlation coefficients and the signal-to-noise ratio was also performed.